Front. Chem. Sci. Eng. 2020, 14(6): 1065–1071
https://doi.org/10.1007/s11705-019-1909-x

RESEARCH ARTICLE

Effect of electrolyte concentration on the tribological performance of MAO coatings on aluminum alloys

Chao Wang (✉)[1*], Jun Chen[1,2*], Jihua He[1], Jing Jiang[1], Qinyong Zhang[2]

1 Clean Energy Materials and Engineering Center, State Key Laboratory of Electronic Thin Film and Integrated Device, School of Electronic Science and Engineering, University of Electronic Science and Technology of China, Chengdu 611731, China
2 School of Materials Science and Engineering, Xihua University, Chengdu 610039, China

Abstract Micro-arc oxidation (MAO) is an efficient approach to improve the hardness, wear resistance, and other properties of aluminum alloys. In order to investigate the effect of the electrolyte concentration on the properties of MAO coatings for LY12 alloy, the voltage variation during the MAO process was recorded. The surface morphologies and phase compositions of the coatings produced with different electrolytes were investigated using scanning electron microscopy and X-ray diffraction, respectively. The roughness and thickness of the coatings were measured using a pocket roughness meter and an eddy-current thickness meter, respectively. The tribological performances of the coatings were investigated against GCr15 bearing steel on a ball-on-disc wear tester in open air. The results showed that with an increase in the Na_2SiO_3 content, the working voltage of the MAO process decreased, the roughness and thickness of the coatings increased significantly, and the relative content of the α-Al_2O_3 phase decreased. With an increase in the KOH content, the working voltage decreased slightly, the roughness and thickness of the coatings increased slightly, and the α- and γ-Al_2O_3 phase contents remained unchanged. The friction coefficient and wear rate of the coatings increased with an increase in the Na_2SiO_3 and KOH concentrations. A decrease in the porosity and roughness and an increase in the α-Al_2O_3 content of the coatings reduced their wear mass loss.

Keywords aluminum alloy, micro-arc oxidation, coating, electrolyte concentration, tribological performance

1 Introduction

Al alloys are ideal for applications in the aerospace, automobile, and military industries. However, Al alloys often show poor tribological performance because of their low hardness [1,2]. In order to improve the wear resistance of Al alloys, various surface treatment methods have been developed. Micro-arc oxidation (MAO) is considered to be a promising method for depositing protective films on the surface of Al alloys. This technique has been extensively used for depositing ceramic coatings on the surface of valve metals such as Mg, Al, and Ti and their alloys [3–13]. The *in-situ* formation of MAO coatings improves the bonding strength of alloys [14] and protects the substrate during the friction process. For Al alloys in particular, it is relatively easier to form coatings with extremely high hardness by adjusting the MAO parameters. Such ceramic coatings improve the integral performance of Al substrates [15–17].

The quality of MAO coatings (microstructure, composition, and performance) is affected by many factors including the composition and concentration of the electrolyte. MAO coatings are mainly prepared using alkaline electrolytes. This is because MAO coatings prepared using alkaline electrolytes exhibit favorable properties. For example, Rehman et al. found that the hardness and wear properties of MAO coatings are superior to those of the coatings prepared without NaOH addition or with NaOH amounts higher than 2 $g \cdot L^{-1}$ [18]. Solutions based on silicates increase the intensity of sparking discharge and improve the cohesive properties of MAO coatings [19]. Hence, alkaline and silicate electrolytes are widely used for preparing MAO coatings. Various studies have been carried out to investigate the effect of the electrolyte composition on the performance of MAO coatings [18–23]. However, very few studies have been carried out to compare the effects of various additives on

Received August 9, 2019; accepted November 1, 2019

E-mail: cwang@uestc.edu.cn

*These authors contributed equally to this work.

the properties of MAO coatings.

In this study, MAO coatings were fabricated on the surface of LY12 alloy in the presence of electrolytes with different Na_2SiO_3 and KOH concentrations. The effects of each electrolyte additive on the tribological performance of the MAO coatings were investigated. The relationship between the working voltage and deposition time of the MAO coatings with different concentrations was investigated. The microstructures, phase compositions, thickness, and roughness of the MAO coatings formed using different electrolytes were investigated. The tribological performances (friction coefficient, mass loss) of the MAO coatings were also evaluated.

2 Experimental

2.1 MAO treatment

LY12 alloy sheets with the dimensions of 20 mm × 20 mm × 3 mm were used as the substrates for the MAO treatment. The nominal composition of the alloy in weight percentage was 3.8%–4.9% Cu, 0.3%–0.7% Mn, 0.5%–1.8% Mg, 0.5% Fe, 0.5% Si, 0.1% Cr, 0.25% Zn, 0.1% Ti, and Al balance. A bipolar pulse electrical power of 20 kW was employed. The equipment consisted of a voltage transformer, an AC power supply, an electrolyte cell, a stirring system, a cooling system, and other affiliated components. Prior to the MAO treatment, the samples were ground with a 1200-grit SiC paper and then ultrasonically cleaned with distilled water and acetone. The sheets were used as the anode and a water-cooled electrolyzer made up of stainless steel served as the cathode. The reaction temperature was maintained at 20°C–30°C by adjusting the stirring and the flow of the cooling water. A constant current density of 10 $A \cdot dm^{-2}$ was maintained at the substrate surface for 60 min by controlling the voltage pulses during the MAO process. The pulse frequency was set at 300 Hz. Table 1 lists the Na_2SiO_3 and KOH concentrations of the MAO coatings prepared in this study. The basic electrolyte consisted of distilled water along with Na_2SiO_3 (5 $g \cdot L^{-1}$) and KOH (0.5 $g \cdot L^{-1}$) as the main film-forming agents. In order to investigate the effect of the Na_2SiO_3 concentration on the tribological performance of the MAO coatings, the concentration of KOH was kept constant at 0.5 $g \cdot L^{-1}$. Similarly, for investigating the effect of the KOH concentration, the concentration of Na_2SiO_3 was kept constant at 5 $g \cdot L^{-1}$. Three samples S1, S2, and S3 were prepared using the electrolytes containing 5, 10 and 15 $g \cdot L^{-1}$ of Na_2SiO_3, respectively. Three samples S1, S4, and S5 were prepared using the electrolytes containing 0.5, 1.0 and 1.5 $g \cdot L^{-1}$ of KOH, respectively.

Table 1 MAO coatings formed using electrolytes with different concentrations of Na_2SiO_3 and KOH

Specimens	S1	S2	S3	S4	S5
Concentrations of Na_2SiO_3/($g \cdot L^{-1}$)	5	10	15	5	5
Concentrations of KOH/($g \cdot L^{-1}$)	0.5	0.5	0.5	1.0	1.5

2.2 Characterization

The phase compositions of the coatings were analyzed using X-ray diffraction (XRD, PANalytical, EMPRYR-EAN series 2, Netherlands) with a Cu target. The morphologies of the specimens were examined using scanning electron microscopy (SEM, KYKY, EM3200, Beijing) and energy dispersive X-ray spectroscopy (EDS). The roughness (R_a) of the MAO coatings was determined using a pocket roughness meter (TR110, Beijing). Five spots were tested on both the sides of the ceramic coatings and a mean value of R_a was recorded. The thickness of the coatings was measured using an eddy-current thickness meter (QNIX 4200/4500, Automation, Germany). The average value obtained from the thickness values at five spots (on each side) was reported.

In order to investigate the tribological performances of the MAO coatings, their friction and wear tests were carried out using a ball-on-disc wear tester (HT-1000, Lanzhou). The counterface material was a GCr15 bearing steel ball with a diameter of 6 mm and a hardness of about 62 HRC. The tests were carried out at room temperature under the dry friction condition at a load of 500 g with a rotation radius of 2 mm at a sliding speed of 560 $r \cdot min^{-1}$. The samples were ultrasonically washed for 5 min with acetone before weighing. The wear mass loss of the specimens was calculated using a BSA224S analytical balance.

3 Results and discussion

3.1 Behavior of the MAO process

Figure 1 shows the voltage-time responses of the coatings prepared using the electrolytes with different concentrations of Na_2SiO_3 and KOH. All the five specimens showed similar voltage-time responses. The voltage-time curves of all the specimens showed two stages. In the beginning, the voltage increased to more than 400 V in a linear progression within 3 min. This rapid voltage increase can be attributed to the rapid coating growth during this stage. Many small luminescent sparks were uniformly distributed on the surface of the specimens and moved quickly around the break-down voltage of the coatings. Then, the voltage increased slowly with the final voltage for the all specimens reaching above 500 V.

The final voltages of S1, S2, S3, S4 and S5 (Figs. 1(a) and 1(b)) were 546, 531, 515, 537 and 529 V, respectively. This indicates that with an increase in the Na_2SiO_3 and KOH concentrations, the voltage of the MAO coatings

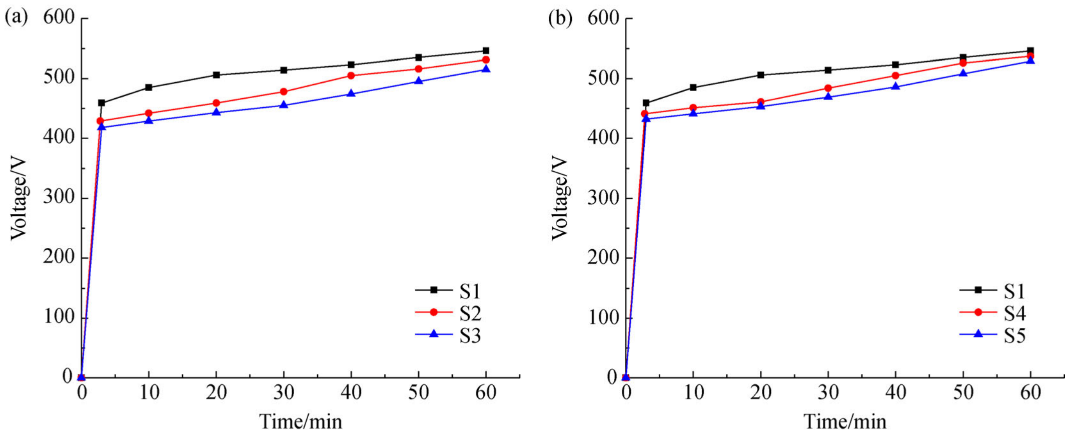

Fig. 1 Voltage-time responses of the coatings prepared using the electrolytes with different concentrations of (a) Na_2SiO_3 and (b) KOH.

decreased. This is because with the addition of the electrolyte, the resistance and potential drop of the solution decreased and the potential drop of the samples increased. As a result, the effective energy working on the samples increased and the energy consumption of the MAO process decreased. Hence, the coatings with lower additive concentrations showed higher voltages. Similar phenomenon has been reported previously for coatings prepared using electrolytes containing Na_2SiO_3. An increase in the Na_2SiO_3 concentration increased the electrolyte conductivity and decreased the positive final voltage [19].

3.2 Microstructure characterization

The surface morphologies of the ceramic coatings formed using the electrolytes with different concentrations of Na_2SiO_3 and KOH are shown in Fig. 2. The surface of S1 showed cake-like formations. This is because at the high temperatures and under high pressures, the melted oxides erupted with intensive sparking around the discharge channels. These oxides deposited on the surface and then solidified in the cold electrolyte when the sparks went out. At low Na_2SiO_3 concentrations, the weak discharge made

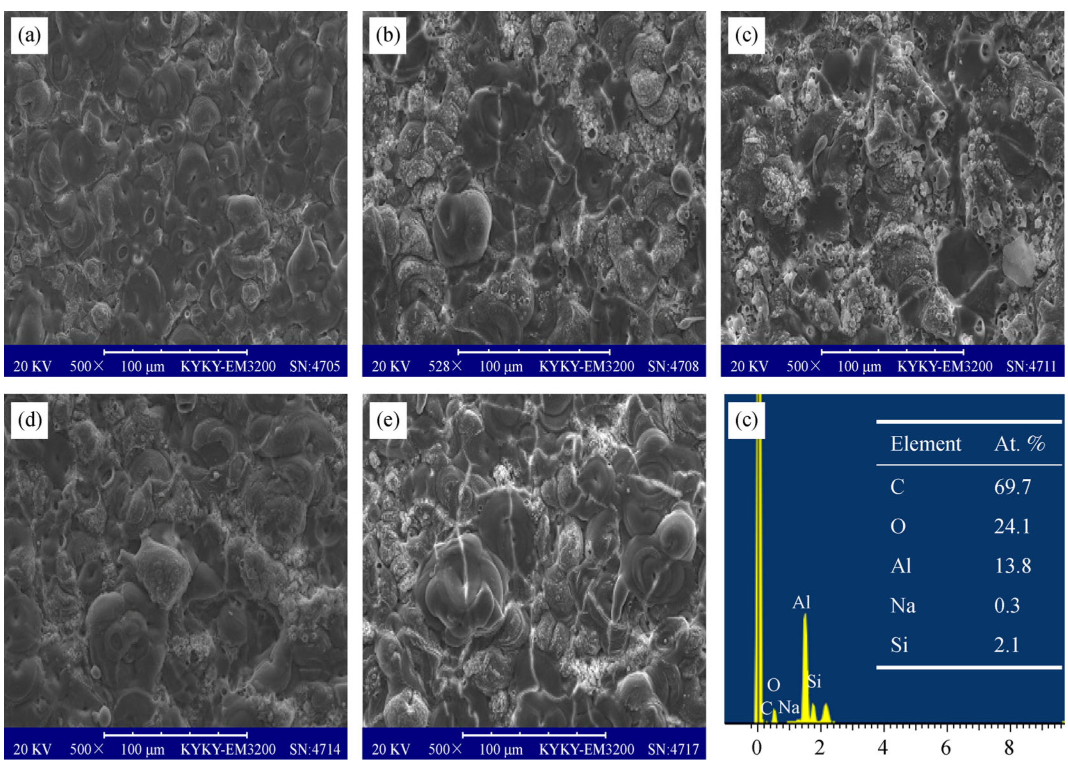

Fig. 2 Surface micrographs of the MAO coatings formed using the electrolytes with different concentrations of Na_2SiO_3 and KOH: (a) S1, (b) S2, (c) S3, (d) S4, (e) S5 and (f) the EDS mapping of S3.

the erupting melted oxides solidify rapidly and cover the discharge channels. Hence, S1 showed a smooth surface. Pores could hardly be observed on this surface. With an increase in the Na_2SiO_3 concentration, the conductivity of the electrolyte increased, which accelerated the MAO process and increased the discharge intensity. As a result, the surface quality of S2 worsened. Many particles were distributed around the cakes with pores of different sizes, and cracks ran through the cakes. With a further increase in the Na_2SiO_3 concentration (S3), the surface became much looser and more inhomogeneous with larger pores, and a large number of particles with different sizes piled up around the discharging channels. The conductivity of the electrolyte also increased with an increase in the KOH concentration. Compared to S1, S4 and S5 showed uneven surfaces because of the accumulation of oxide particles. The cake-like blocks accumulated and transformed into a flower-like structure, indicating that even a small increase in the KOH concentration made the surface of the coatings rough.

All the samples showed similar EDS mappings. Therefore, only the EDS mapping of S3 is shown in Fig. 2(f). This sample mainly consisted of O and Al. The presence of C in the sample can be attributed to the adventitious hydrocarbons present in the environment. This sample showed traces of Na and the largest amount of Si among all the samples because of its highest Na_2SiO_3 content.

Table 2 lists the surface roughness values of the MAO coatings prepared using the electrolytes with different concentrations of Na_2SiO_3 and KOH. The sample with the lowest Na_2SiO_3 and KOH concentrations showed the lowest surface roughness, which steadily increased with an increase in the Na_2SiO_3 and KOH concentrations. These results are consistent with the SEM results reported by Zong et al. They demonstrated that the compactness of MAO coatings is affected by the roughness of their surface [24].

Table 2 Roughness of the MAO coatings

Specimens	S1	S2	S3	S4	S5
R_a/μm	1.56	2.73	3.94	1.94	2.57

3.3 Phase composition

Figure 3 shows the XRD patterns of the coatings formed using different Na_2SiO_3 and KOH concentrations. The coatings were mainly composed of the α-Al_2O_3 and γ-Al_2O_3 phases, and the Al phase originated from the substrate. No diffraction peaks corresponding to silicides were observed, although the EDS results indicated the presence of Si. This can be attributed to the low concentration and amorphous state of Si in the coatings. It can be observed from Fig. 4(a) that the non-crystallinity of the coatings increased with an increase in the Na_2SiO_3 concentration. This is consistent with the SEM results. Hence, the nodular structure became predominant with an increase in the Na_2SiO_3 concentration. In addition, the intensity of the α-Al_2O_3 peak decreased gradually with an increase in the Na_2SiO_3 concentration, indicating that Na_2SiO_3 inhibited the transformation of γ-Al_2O_3 into α-Al_2O_3. This can be attributed to the final voltages of the samples with different Na_2SiO_3 concentrations. Cubic γ-Al_2O_3 and hexagonal close-packed α-Al_2O_3 are thermodynamically metastable and stable alumina phases, respectively [25]. With an increase in the Na_2SiO_3 concentration, voltage decreased, resulting in a decrease in temperature and pressure during the MAO process, which prevented the transformation of γ-Al_2O_3 into a more stable form. This is consistent with the results reported by Weng et al., who pointed out that the thermodynamically stable α-Al_2O_3 phase can be formed at high temperatures, while the γ-Al_2O_3 phase is formed by rapid cooling [26]. Hence, the MAO ceramic coating with 5 $g\cdot L^{-1}$ Na_2SiO_3 showed good crystallinity.

On the other hand, the MAO coatings with different KOH concentrations exhibited similar α-Al_2O_3 and γ-Al_2O_3 peak intensities. This is because the difference

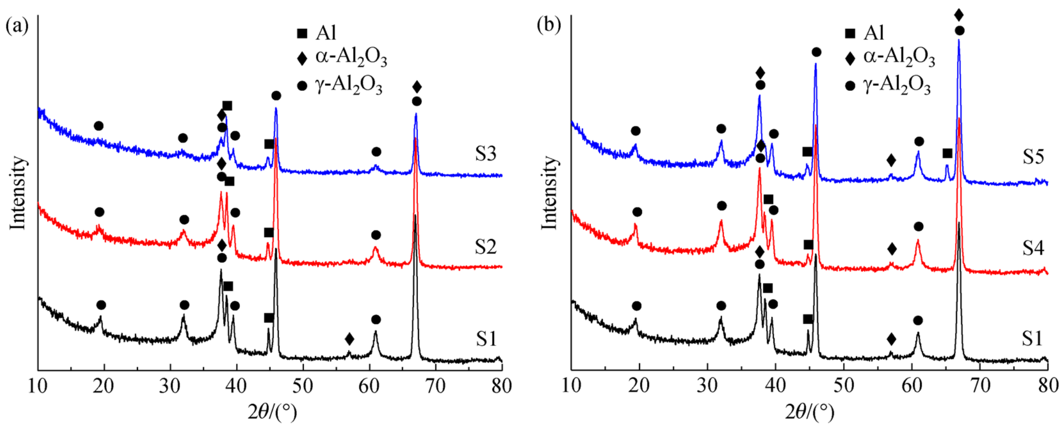

Fig. 3 X-ray diffraction patterns of the coatings prepared using the electrolytes with different concentrations of (a) Na_2SiO_3 and (b) KOH.

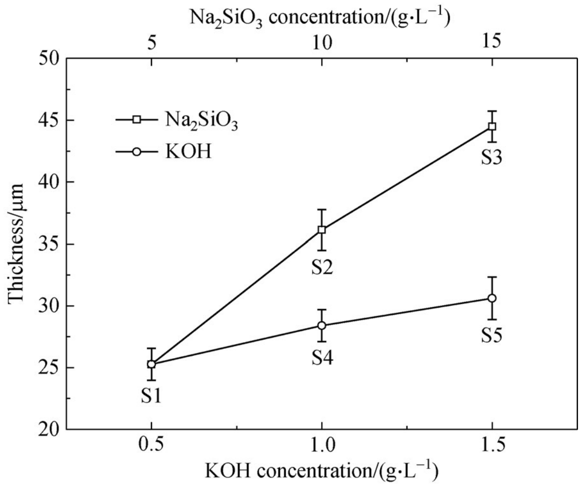

Fig. 4 Thickness of the MAO coatings formed using the electrolytes with different concentrations of Na_2SiO_3 and KOH.

in the KOH concentrations was small. Therefore, the KOH concentration showed little effect on the crystallinity of the ceramic coatings.

3.4 Coating thickness

The thickness of the coatings formed using the electrolytes with different Na_2SiO_3 and KOH concentrations was measured using an eddy-current thickness meter (Fig. 4). The coating thickness increased rapidly with an increase in the Na_2SiO_3 concentration, while it increased slowly with an increase in the KOH concentration. The increase in the Na_2SiO_3 concentration resulted in the reinforcement of the electrolyte conductivity, thus enhancing the discharge intensity during the MAO process. Thus, a large number of SiO_3^{2-} ions moved toward the surface of the anode under the action of the electric field and entered the discharge channels to participate in the reaction [27]. Therefore, an increase in the Na_2SiO_3 concentration increased the thickness of the coatings. With an increase in the KOH concentration, the arcing voltage decreased, thus accelerating the formation of the coatings. However, KOH is highly alkaline. The following chemical reaction occurs during the MAO process: $Al_2O_3 + 2KOH = 2KAlO_2 + H_2O$. Hence, in this study, we used low KOH concentrations. The thickness of the coatings increased slightly with an increase in the KOH concentration. Although the S3 coating showed the highest thickness owing to its highest Na_2SiO_3 concentration, it showed the loosest microstructure. It can be attributed to the occurrence of an intensive micro discharge, which released a large amount of energy on the thick coating. This led to the formation of structural defects, which loosened the structure of the coating [19].

3.5 Friction and wear properties of the coatings

Figure 5 shows the friction coefficient of the samples prepared using different Na_2SiO_3 and KOH concentrations as a function of time. The friction coefficients of S1, S2, S3, S4 and S5 were 0.58, 0.61, 0.71, 0.72 and 0.75, respectively. The S1 coating exhibited the lowest friction coefficient, and the curve of friction coefficient was in low volatility. The friction coefficient of the coatings increased with an increase in the Na_2SiO_3 and KOH concentrations. The surface roughness of a material significantly affects its friction coefficient. As can be observed from Table 2, S1 showed the lowest roughness. Therefore, S1 showed the lowest friction coefficient. Moreover, during the initial 150 s of the friction test, the friction coefficients of S4 and S5 were lower than those of S2 and S3 (as expected) because of the lower roughness of S2 and S3. However, the friction coefficients of S4 and S5 increased rapidly with strong vibration when the friction was applied for longer durations. The friction coefficient of S5 increased suddenly to about 0.7 after 500 s. This can be attributed to the partial peeling off of the coating material during the friction coefficient test. The particles of the MAO coating increased the friction coefficient. This indicates that the KOH concentration significantly affected the friction coefficient of the coatings.

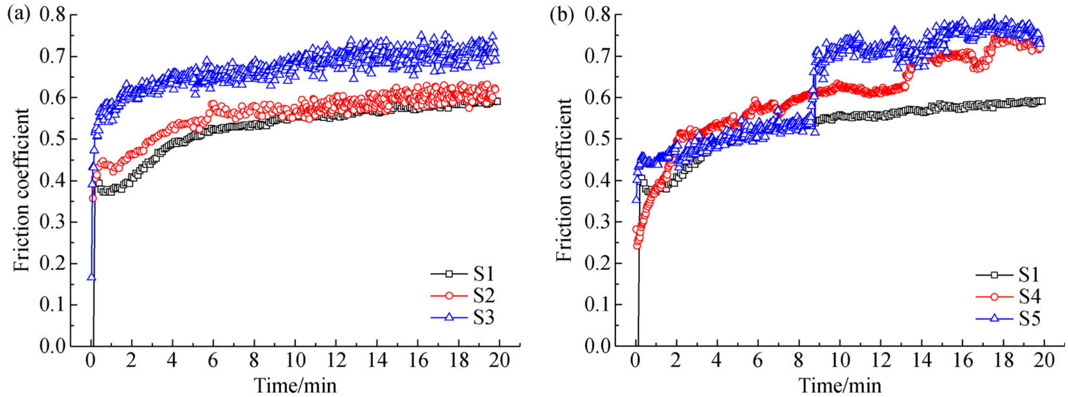

Fig. 5 Friction coefficients of the MAO coatings formed using the electrolytes with different concentrations of (a) Na_2SiO_3 and (b) KOH.

Table 3 lists the average wear mass loss of the five samples and the Al substrate tested against the GCr15 bearing steel ball in air for 20 min. The mass loss of the untreated Al substrate was much higher than those of the five MAO-coated samples. S1 showed similar mass losses before and after the friction and wear tests, exhibiting excellent wear resistance. An increase in the Na_2SiO_3 and KOH concentrations deteriorated the anti-wear properties of the samples. It can be concluded that the wear resistance of the coatings was affected not only by their thickness, but also by the changes in their phase compositions and surface characteristics. It has been reported that an increase in the α-Al_2O_3 phase content increases the hardness and improves the wear resistance of coatings [25,28]. Apart from the hardness, the friction coefficient is another key factor affecting the wear resistance of MAO coatings. Hence, the wear mass losses of S2 and S3 increased with an increase in the Na_2SiO_3 concentration.

Table 3 Wear mass loss of the coatings

Specimens	S1	S2	S3	S4	S5	Al substrate
Wear mass loss/mg	0.1	0.3	0.4	0.3	0.5	3.2

S5 showed larger wear mass loss than S3 although it showed a phase composition similar to that of S1 and a surface roughness lower than that of S3. This can be attributed to the increase in the friction coefficient of the sample with an increase in the friction test duration. The MAO coatings could efficiently protect the Al substrate. The wear mass loss of the samples with the MAO coatings was about ten times lower than that of the bare Al alloy. Hence, the wear loss resistance of the coatings developed in this study was much higher than those of the previously reported coatings (which only doubled the wear loss resistance of the substrate) [18].

4 Conclusions

In this study, ceramic coatings were fabricated on the surface of LY12 alloy via MAO. The effects of the electrolyte concentration on the properties of the MAO coatings were investigated. The working voltage decreased with an increase in the Na_2SiO_3 and KOH concentrations. The surface of the coating formed using the electrolyte containing 5 $g \cdot L^{-1}$ Na_2SiO_3 and 0.5 $g \cdot L^{-1}$ KOH (S1) was smooth and showed low porosity. With an increase in the Na_2SiO_3 concentration, the roughness and thickness of the coatings increased significantly, while the relative content of the α-Al_2O_3 phase decreased. With an increase in the KOH concentration, the roughness and thickness of the ceramic coatings increased slightly, while their composition remained almost the same.

The MAO coatings exhibited good anti-wear resistance. Both the friction coefficient and wear rate of the coatings increased gradually with an increase in the Na_2SiO_3 and KOH concentrations. The wear mass loss of the S1 coating was only 0.1 mg, which represented the best tribological property. The results showed that the wear resistance of the coatings depended on their phase composition and friction coefficient and not on the coating thickness.

Acknowledgements This work was supported by the China Postdoctoral Science Foundation Funded Project (No. 2016M602668), the Fundamental Research Funds for the Central Universities of University of Electronic Science and Technology of China (No. ZYGX2015J029), the Project of the Science and Technology Department in Sichuan Province Supporting Plan (No. 2016JQ0022) and the National Natural Science Foundation of China (Grant No. 51501156).

References

1. Buldum B B, Bayhan B. Effect of ball-burnishing parameters on surface roughness and surface hardness of aluminum alloy 6013. Materials Testing, 2018, 60(4): 418–422
2. Miller W S, Zhuang L, Bottema J, Wittebrood A J, De Smet P, Haszler A, Vieregge A. Recent development in aluminium alloys for the automotive industry. Materials Science and Engineering A, 2000, 280(1): 37–49
3. Nie X, Meletis E I, Jiang J C, Leyland A, Yerokhin A L, Matthews A. Abrasive wear/corrosion properties and TEM analysis of Al_2O_3 coatings fabricated using plasma electrolysis. Surface and Coatings Technology, 2002, 149(2–3): 245–251
4. Yang X, Chen L, Jin X Y, Du J C, Xue W B. Influence of temperature on tribological properties of microarc oxidation coating on 7075 aluminium alloy at 25°C–300°C. Ceramics International, 2019, 45(9): 12312–12318
5. Lv X C, Cao L, Wan Y, Xu T W. Effect of different electrolytes in micro-arc oxidation on corrosion and tribological performance of 7075 aluminum alloy. Materials Research Express, 2019, 6(8): 086421
6. Yilmaz M S, Sahin O. Applying high voltage cathodic pulse with various pulse durations on aluminium via micro-arc oxidation (MAO). Surface and Coatings Technology, 2018, 347: 278–285
7. Gu Y, Ma H, Yue W, Tian B, Chen L L, Mao D. Microstructure and corrosion model of MAO coating on nano grained AA2024 pretreated by ultrasonic cold forging technology. Journal of Alloys and Compounds, 2016, 681: 120–127
8. Nasiri-Vatan H, Ebrahimi-Kahrizsangi R, Asgarani M K. Tribological performance of PEO-WC nanocomposite coating on Mg alloys deposited by plasma electrolytic oxidation. Tribology International, 2016, 98: 253–260
9. Yavari S A, Necula B S, Fratila-Apachitei L E, Duszczyk J, Apachitei I. Biofunctional surfaces by plasma electrolytic oxidation on titanium biomedical alloys. Surface Engineering, 2016, 32(6): 411–417
10. Yu S R, Yao Q, Chu H C. Morphology and phase composition of MAO ceramic coating containing Cu on Ti_6Al_4V alloy. Rare Metals, 2017, 36(8): 671–675
11. Marques I S V, Alfaro M F, Cruz N C, Mesquita M F, Takoudis C,

Sukotjo C, Mathew M T, Barão V A R. Tribocorrosion behavior of biofunctional titanium oxide films produced by micro-arc oxidation: Synergism and mechanisms. Journal of the Mechanical Behavior of Biomedical Materials, 2016, 60: 8–21
12. Sarbishei S, Faghihi Sani M A, Mohammadi M R. Effects of alumina nanoparticles concentration on microstructure and corrosion behavior of coatings formed on titanium substrate via PEO process. Ceramics International, 2016, 42(7): 8789–8797
13. İzmir M, Ercan B. Anodization of titanium alloys for orthopedic applications. Frontiers of Chemical Science and Engineering, 2019, 13(1): 28–45
14. Li J X, Zhang Y M, Han Y, Zhao Y M. Effects of micro-arc oxidation on bond strength of titanium to porcelain. Surface and Coatings Technology, 2010, 204(8): 1252–1258
15. Lu Z, Ouyang Z, Grant N, Wan Y M, Yan D, Lennon A. Manipulation of stored charge in anodic aluminium oxide/SiO_2 dielectric stacks by the use of pulsed anodisation. Applied Surface Science, 2016, 363: 296–302
16. Tian J, Luo Z Z, Qi S K, Sun X J. Structure and antiwear behavior of micro-arc oxidized coatings on aluminum alloy. Surface and Coatings Technology, 2002, 154(1): 1–7
17. Xin S G, Song L X, Zhao R G, Hu X F. Properties of aluminium oxide coating on aluminium alloy produced by micro-arc oxidation. Surface and Coatings Technology, 2005, 199(2-3): 184–188
18. Rehman Z U, Lee D G, Koo B H. Effect of OH− concentration on the mechanical and microstructural properties of microarc oxidatoin coating produced on Al7075 alloy. Korean Journal of Materials Research, 2015, 25(10): 503–508
19. Polat A, Makaraci M, Usta M. Influence of sodium silicate concentration on structural and tribological properties of microarc oxidation coatings on 2017A aluminum alloy substrate. Journal of Alloys and Compounds, 2010, 504(2): 519–526
20. Zheng H, Wang Y, Li B, Han G R. The effects of Na_2WO_4 concentration on the properties of microarc oxidation coatings on aluminum alloy. Materials Letters, 2005, 59(2-3): 139–142
21. Jin F, Chu P K, Tong H, Zhao J. Improvement of surface porosity and properties of alumina films by incorporation of Fe micrograins in micro-arc oxidation. Applied Surface Science, 2006, 253(2): 863–868
22. Tseng C C, Lee J L, Kuo T H, Kuo S N, Tseng K H. The influence of sodium tungstate concentration and anodizing conditions on microarc oxidation (MAO) coatings for aluminum alloy. Surface and Coatings Technology, 2012, 206(16): 3437–3443
23. Wang P, Wu T, Peng H, Yang G X. Effect of $NaAlO_2$ concentrations on the properties of micro-arc oxidation coatings on pure titanium. Materials Letters, 2016, 170: 171–174
24. Zong Y, Song R G, Hua T S, Cai S W, Wang C, Li H. Effects of current frequency on the MAO coatings on AA7050. Surface Engineering, 2019: 1–8
25. Barati N, Meletis E I, Golestani Fard F, Yerokhin A, Rastegari S, Al Faghihi-Sani M A. Al_2O_3-ZrO_2 nanostructured coatings using DC plasma electrolyticoxidation to improve tribological properties of Al substrates. Applied Surface Science, 2015, 356: 927–934
26. Weng Y C, Liu H X, Ji S P, Huang Q, Wu H, Li Z B, Wu Z Z, Wang H Y, Tong L P, Fu R K Y, Chu P K, Pan F. A promising orthopedic implant material with enhanced osteogenic and antibacterial activity: Al_2O_3-coated aluminum alloy. Applied Surface Science, 2018, 457: 1025–1034
27. Lv G, Gu W, Chen H, Feng W R, Khosa M L, Li L, Niu E W, Zhang G L, Yang S Z. Characteristic of ceramic coatings on aluminum by plasma electrolytic oxidation in silicate and phosphate electrolyte. Applied Surface Science, 2006, 253(5): 2947–2952
28. Zhuang J J, Guo Y Q, Xiang N, Lu X Y, Hu Q, Song R G. Sliding wear behaviour and microstructure of PEO coatings formed on aluminium alloy. Materials Science and Technology, 2016, 32(15): 1559–1566